Turning Noise into Signal
A case study at Limburg, Netherlands - a candidate site for ET

Soumen Koley
Maria Bader
Jo van den Brand
Henk Jan Bulten

Nikhef, Amsterdam
skoley@nikhef.nl

Nikhef

Why build the Einstein Telescope?

Einstein Telescope, a 3rd generation GW detector will improve the current adLigo sensitivity by a factor 10 and also improve the detector sensitivity upto low frequencies of 2 Hz.

Advantages of building ET

- An improved detector sensitivity by a factor 10 - *enables a $\mathbf{10^3}$ times larger volume of the universe to be observed.*
- Improved sensitivity upto frequencies of 2 Hz - *observation of BBH or BNS events for longer duration.*
- Strong field tests of General Relativity – *SNR >100*.
- Other astronomical and cosmological implications.

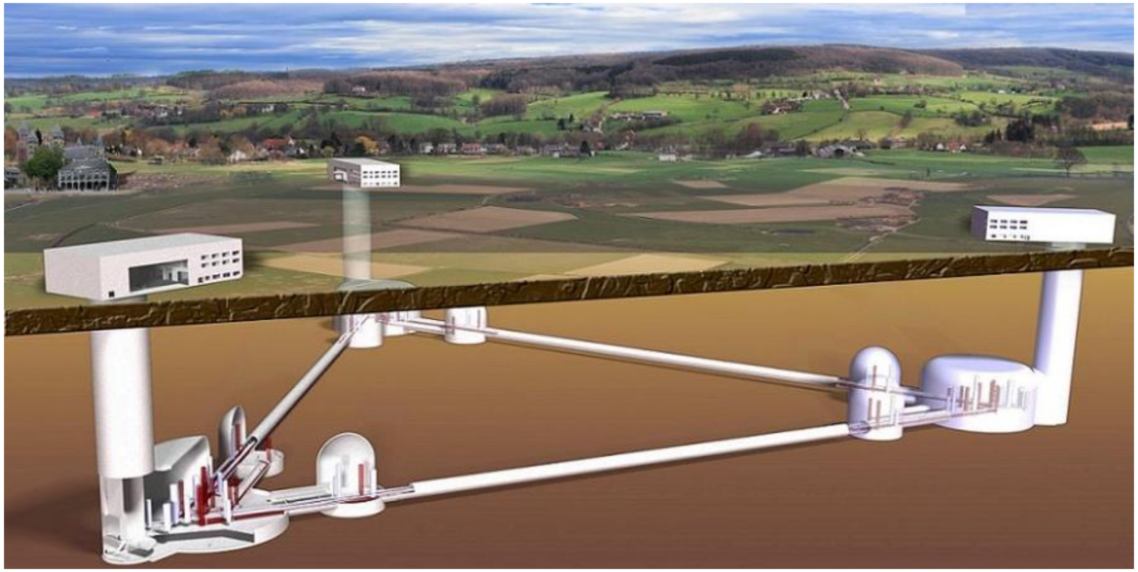

Figure 1. An artists impression of the underground Einstein Telescope GW detector beneath the Limburg landscape.

B-G-NL candidate site for Einstein Telescope

Array and borehole studies are being conducted at the ET candidate site in the Limburg to obtain detailed information about the subsurface.

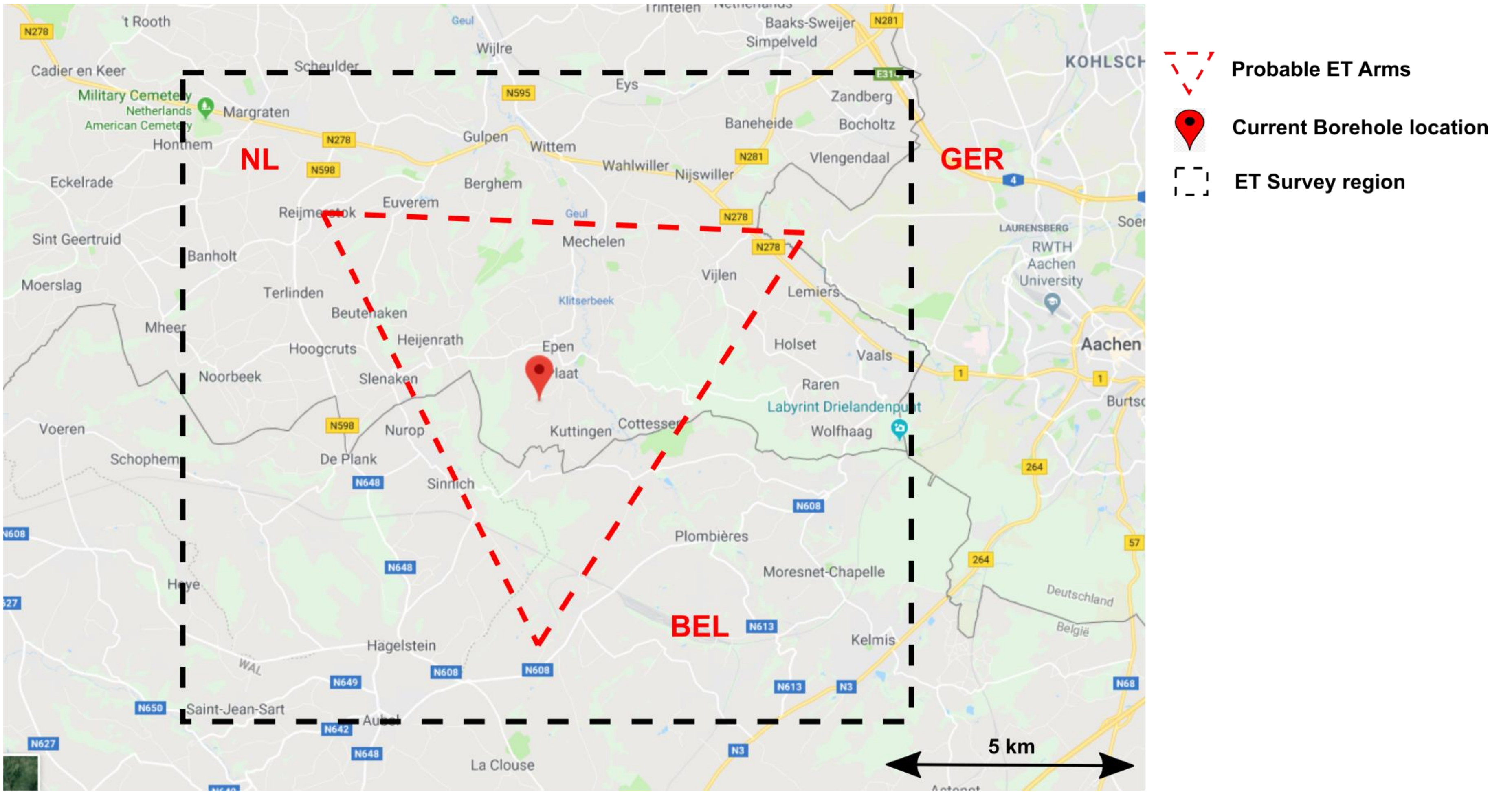

skoley@nikhef.nl

Limiting noise sources for ET

Low frequency sensitivity of ET **may** be limited due to gravity gradient noise also known as Newtonian noise.

Why should ET be built underground?

- Seismic ground motion couple to the suspended elements of the detector through gravitational forces of attraction and cannot be shielded from mechanically.
- Hence only a reduced seismic ground motion can suppress Newtonian noise.
- Ground motion reduces by an order of magnitude as we go deeper (≈ 300 m) in the subsurface. **Hence the need to build ET underground.**

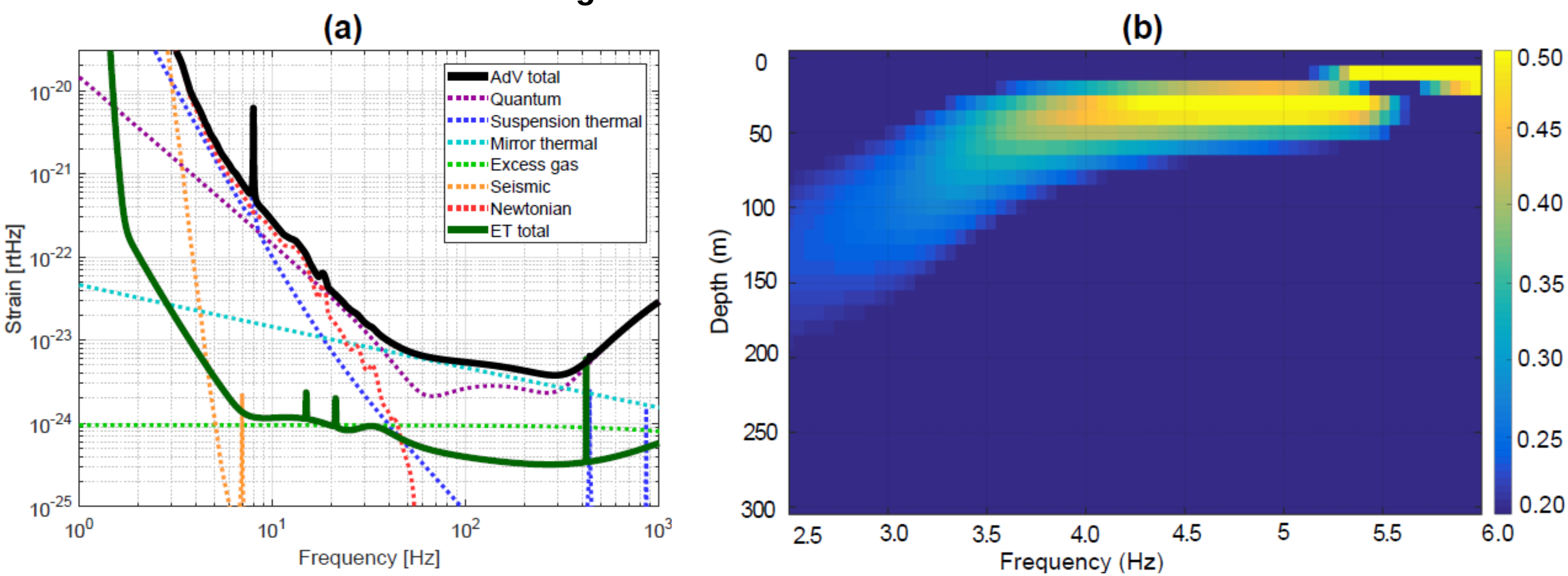

Figure 2(a) AdV noise curves and the ET design sensitivity showing how NN would limit ET sensitivity if built on the earth's surface. (b) Surface wave Eigen function varying with depth and frequency for a Limburg like geology shows the reduced contribution of surface wave seimsic noise at depth.

Inputs to model Newtonian noise

Simulating the subsurface seismic displacement is a necessity for computing the associated Newtonian noise.

Seismic wavefield modeling inputs

- Source mechanism.
- Subsurface parameters like compressional, shear wave velocity, density and quality factor.
- An elastic wave equation solver.

Newtonian noise modeling inputs

- Subsurface displacement.
- Distribution of noise sources.
- Discretizing the simulation domain efficiently.

Newtonian noise subtraction

- Dense array of seismic sensors to measure the seismic noise level.
- Synthesis of ambient seismic wavefield that match our observed ground motions.
- Compute NN and design subtraction schemes.

 skoley@nikhef.nl

Strategies for modeling the subsurface

Subsurface modeling of the subsurface can be carried out using both ***active*** and ***passive*** seismic methods.

Active seismic principle

- Excite the subsurface with a signal of *desired strength and phase* using a vibroseis or an explosive.
- Measure the subsurface response using a array of geophones.
- Use the reflection and refraction response of the subsurface for imaging it.

Passive seismic principle

- Extract the response of the subsurface using the *seismic noise* recorded at multiple geophones.
- Unlike active seismic, measurements of seismic noise needs to be *recorded for long periods* in the range of months to years.
- The dominant contribution of *surface waves* in the recorded seismogram is used to extract the subsurface information.
- **Caveat**
  - Since the response of the medium corresponding to surface waves are studied, this method is sensitive more to changes in shear wave subsurface velocity unlike active seismic which gives a compressional wave velocity model.

Why passive seismic?

- *Less intrusive* and *cheap*.
- Use of wireless geophones enable *flexible sensor geomtery* which helps to study the propagating surface waves in a *desired frequency band* while spanning *huge survey regions*.

Passive seismic interferometry – *stepping stones*

Seismic interferometry is a method of extracting the subsurface response between two geophones by using the simultaneously recorded seismic noise at both the geophones.

A bit of the past:

"*Auto-correlating the transmission response recorded at a receiver on the earth's surface from noise sources in the subsurface, one would retrieve the reflection response at this receiver from a virtual source also at the same location.*" **- Claerbout, 1968**

A bit of nomenclature:

Green's function (GF) response of a medium: A solution to the equation of motion in an elastic solid when the force field is substituted with a delta function defined at a given point in time and space enclosed by the elastic solid.

$$\frac{\partial \tau_{ij}}{\partial x_i} - \frac{\rho \partial^2 u_j}{\partial t^2} = -f_i \qquad \textbf{Equation of motion}$$

Where, τ_{ij} is the stress tensor, u_j is the displacement field, f_i is the external force on the system and $(\mathbf{x}, t)$ are the space and time variable respectively.

Passive seismic interferometry – *the climb*

"Extracting the Green's function response of the medium between two geophones can be understood as a method of cross-correlation of simultaneously recorded seismic noise followed by stacking over many such time segments" – **Wapenaar, 2004**

Seismic interferometry steps:

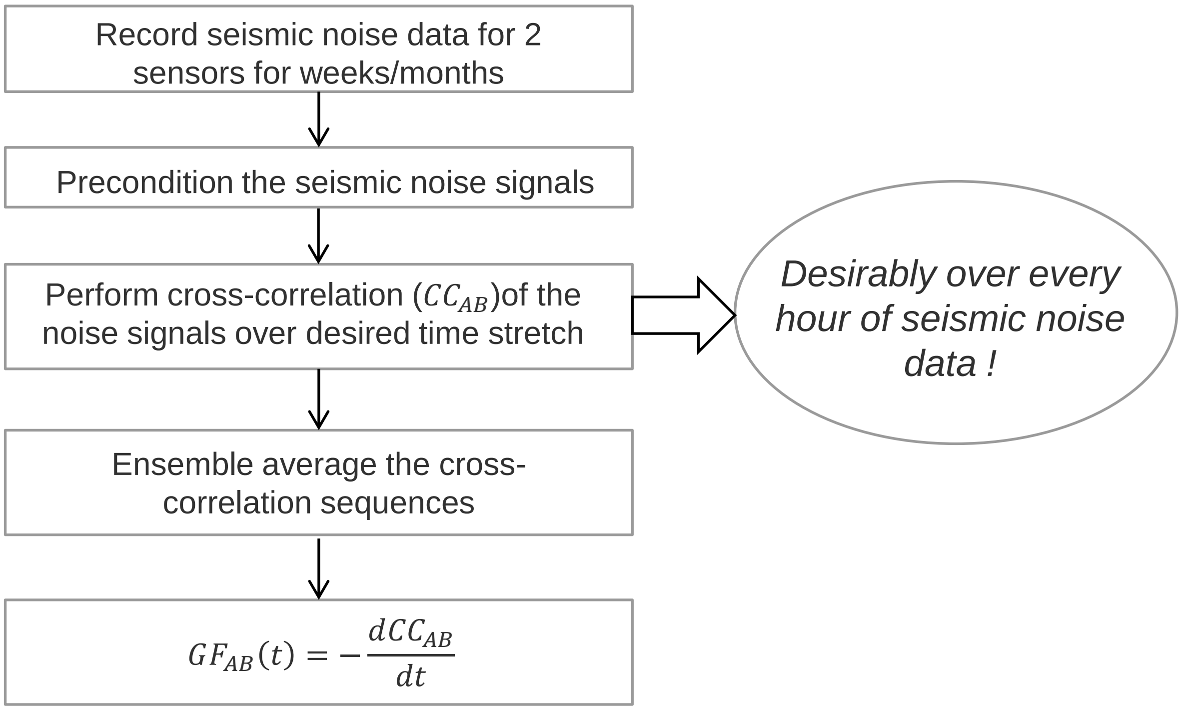

Figure 3. Flowchart showing the steps for performing seismic interferometry.

skoley@nikhef.nl

Seismic noise characteristics – survey 1

Power spectral densities were computed hourly with five minute windows, and then averaged over every day.

Observations

- One order reduction in magnitude of seismic ground motion when measured at 10 m deep compared to the surface.

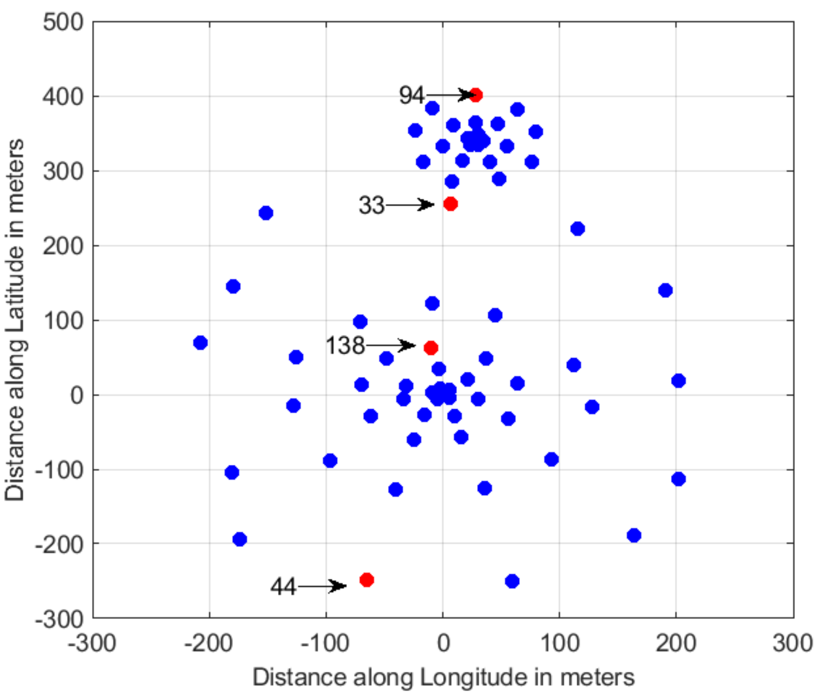

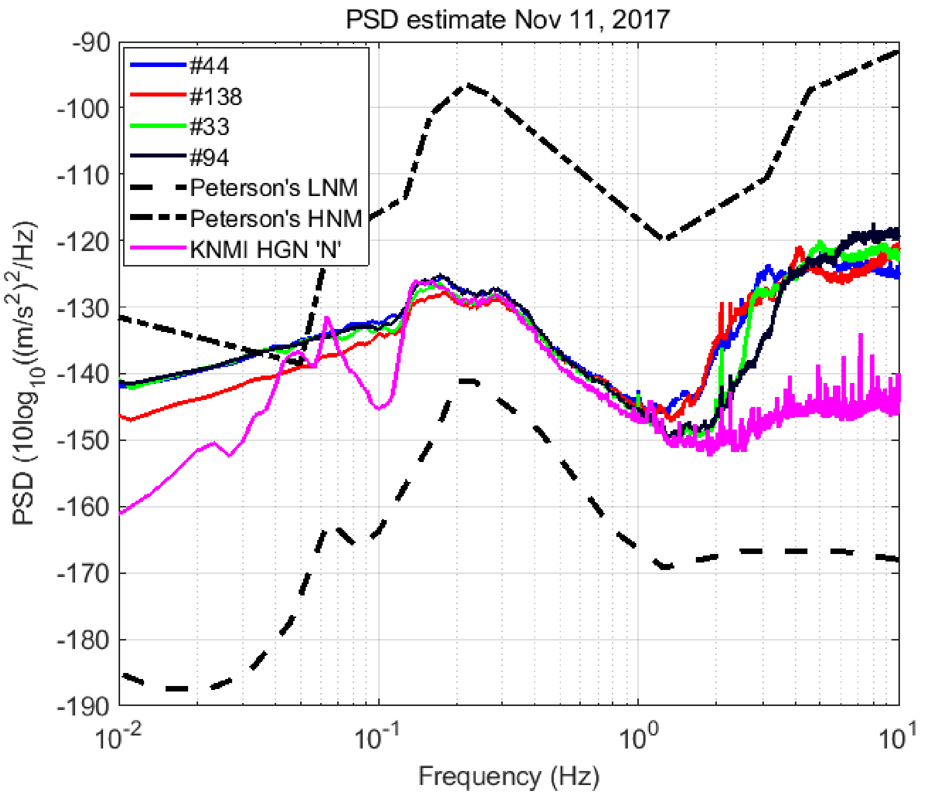

Figure 4(a) Sensor Layout, (b) Daily averaged PSD of sensors for Nov 11, 2017 marked in red

skoley@nikhef.nl

Sensor geometry – *survey 2 for performing 3D subsurface imaging*

146 vertical component geophones deployed along a dense regular grid with consecutive stations separated by ≈ 50 m and the array spanning approximately 950 × 600 sq. m.

Objectives:

- Extract Green's function between every ***possible*** station pair.
- **Why such a dense network?**
  - *Better ray path coverage of the area which enhances the reliability of the tomography results.*

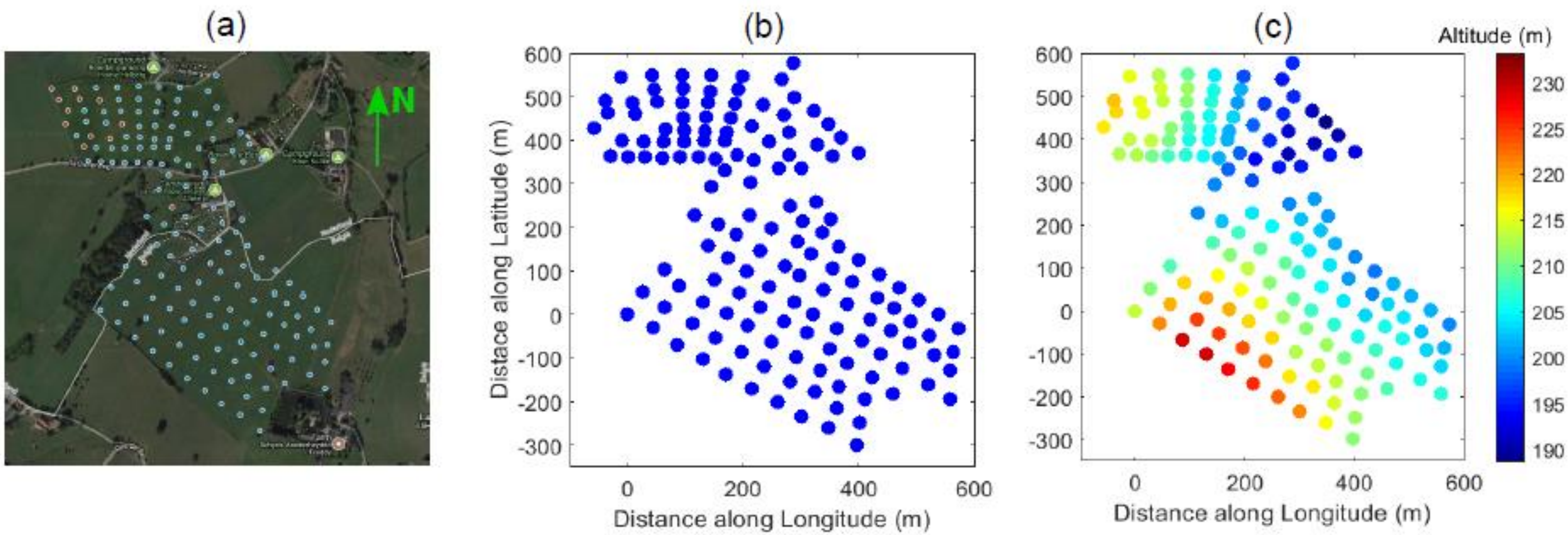

Figure 5 (a) Array geometry on a map of the region. (b) Array layout showing sensor location in cartesian coordinates. (c) Altitude measured at each sensor location shown using the colorbar.

An example Rayliegh wave cross-correlation

We put forth an example of the cross correlation time series between a station pair oriented North-South.

Example

- Figure below shows the daily averaged cross correlation between station # 1009 and 1039 with and without pre-processing of the raw ground motion.

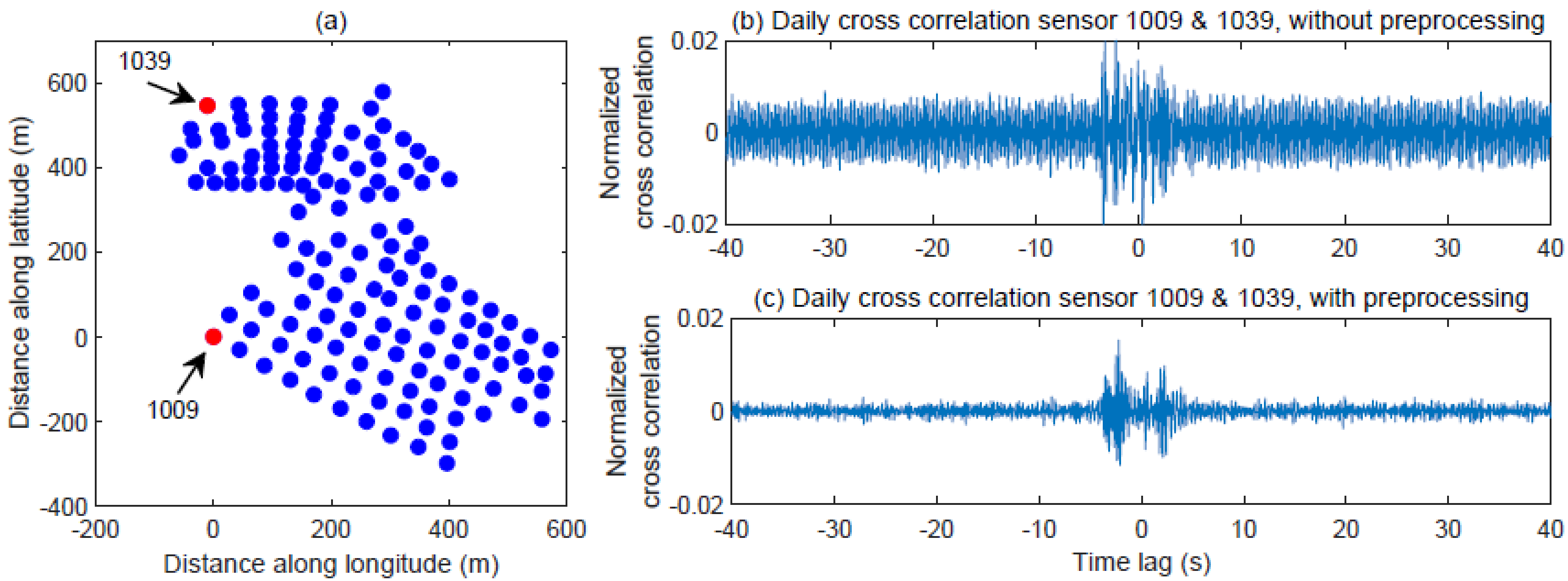

Figure 6(a) Array layout showing the location of sensor 1009 and 1039. (b) Daily cross-correlation time series between sensor 1009 and 1039 without preprocessing. (c) with preprocessing.

skoley@nikhef.nl

Estimating surface wave group velocity – *FTAN analysis*

On extraction of the Green's function from every station pair, we use the frequency-time analysis method (FTAN) to estimate the group velocity of the propagating Rayleigh waves.

Method

- The FTAN method was proposed by Dziewonski et al., 1969 and later formalized by Levshin et al., 1989.
- **FTAN:** computing the signal envelope of the ***symmetric cross correlations*** corresponding to several thin band gaussian filters.
- If $S(f)$ be the fourier transform of the Green's function defined over $\frac{f_{Samp}}{2} \geq f \geq -\frac{f_{Samp}}{2}$, where f_{Samp} is the sampling frequency, then the signal envelope $S_{env}(t)$ in time domain can be computed as,

$$S_{env}(t) = |IFFT\left(S(\omega)\left(1 + sgn(\omega)\right) * G(w, w_0)\right)|$$

- where, $G(\omega, \omega_0)$ is a thin band gaussian filter centred at frequency ω_0.

$$G(\omega, \omega_0) = e^{-\alpha\left(\frac{\omega-\omega_0}{\omega_0}\right)^2}$$

- The modulus of the inverse fourier transformed signal gives us the signal envelope. The maximum of this envelope gives us the group travel time, and hence the group velocity.
- Selecting the value of $\boldsymbol{\alpha}$ is ofcourse subject to the signal strength at different frequencies. For our analysis we used a α between 100 and 200, depending on the SNR of the Green's function.
- A too high value of $\boldsymbol{\alpha}$ might lead to weak SNR, whereas a too high value tends to over-smooth the group velocity estimates, especially at low frequencies where velocity changes are faster.

FTAN at work – *example*

We present here an example of how the FTAN method works for our data set.

Results

- Figures below shows the estimates for station no 110 and 38. Reliable group velocities could only be estimated in the frequency band 2.6-4.5 Hz.
- Since the stations are far apart good correlation was observed only at low frequencies and the correlation magnitudes were significantly low for frequencies > 4.5 Hz.

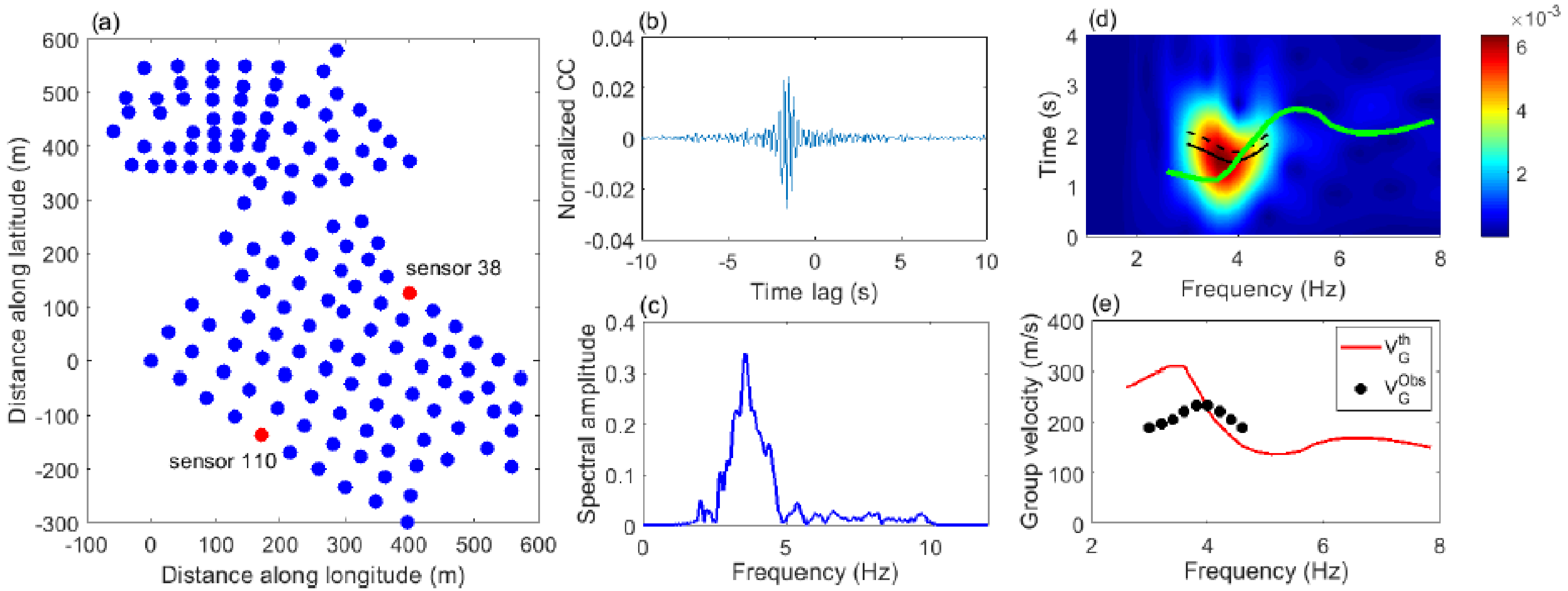

Figure 10. FTAN results for station # 110 and # 38

Group velocity estimates – all station pairs

The FTAN analysis was carried out for all station pairs with a minimum separation of 100 m.

Selection criteria

- Initially a total **10585** CCFs are estimated for all combination of station pairs but a minimum separation of 100 m.
- Group velocity for a particular frequency is only estimated if the station separation is *> 3 times* the wavelength at that frequency *(far field criteria)*
- Out of all station pairs, the pairs that do not lie within the estimated azimuth band obtained from CCBF analysis are discarded. *(Most station pairs that are discarded gives an overestimate of the group velocity as they are not oriented along the dominant noise direction)*.
- **Note**
    - Due to the frequency dependence of the noise direction, it is possible that for a particular station pair some frequencies provide reliable group velocity estimates whereas some not.

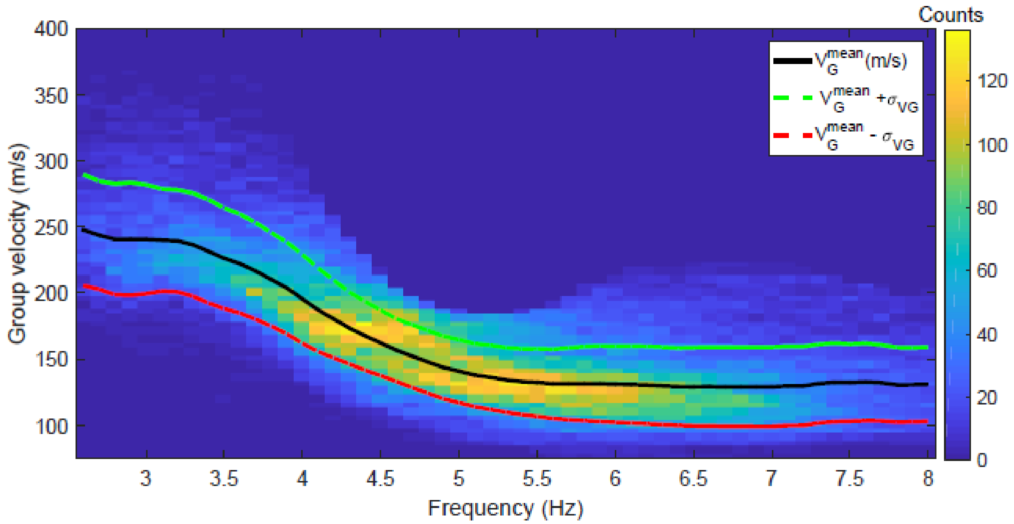

Figure 11. Estimated group velocity histogram as a function of frequency anf the mean group velocity shown with the solid line.

Passive seismic tomography – *checkerboard tests*

Velocities in the simulation domain is made to vary high-low alternately and using the fixed station paths between sensors we aim to reconstruct the checkerboard models back.

Inputs:

- Based on the mean group velocity at each frequency we construct a checker borad velocity model at each frequency with velocity alternating between $v(f)_{gMean} \pm \sigma(f)$ with each square of the size 100 × 100 m.
- **Ray paths** that were found useful from the CCBF method are only used for reconstructing the checker board model.
- A perfect reconstruction is achieved except at frequencies > 5.6 Hz where the south-west corner of the survey region is not reconstructed due to insufficient ray coverage.

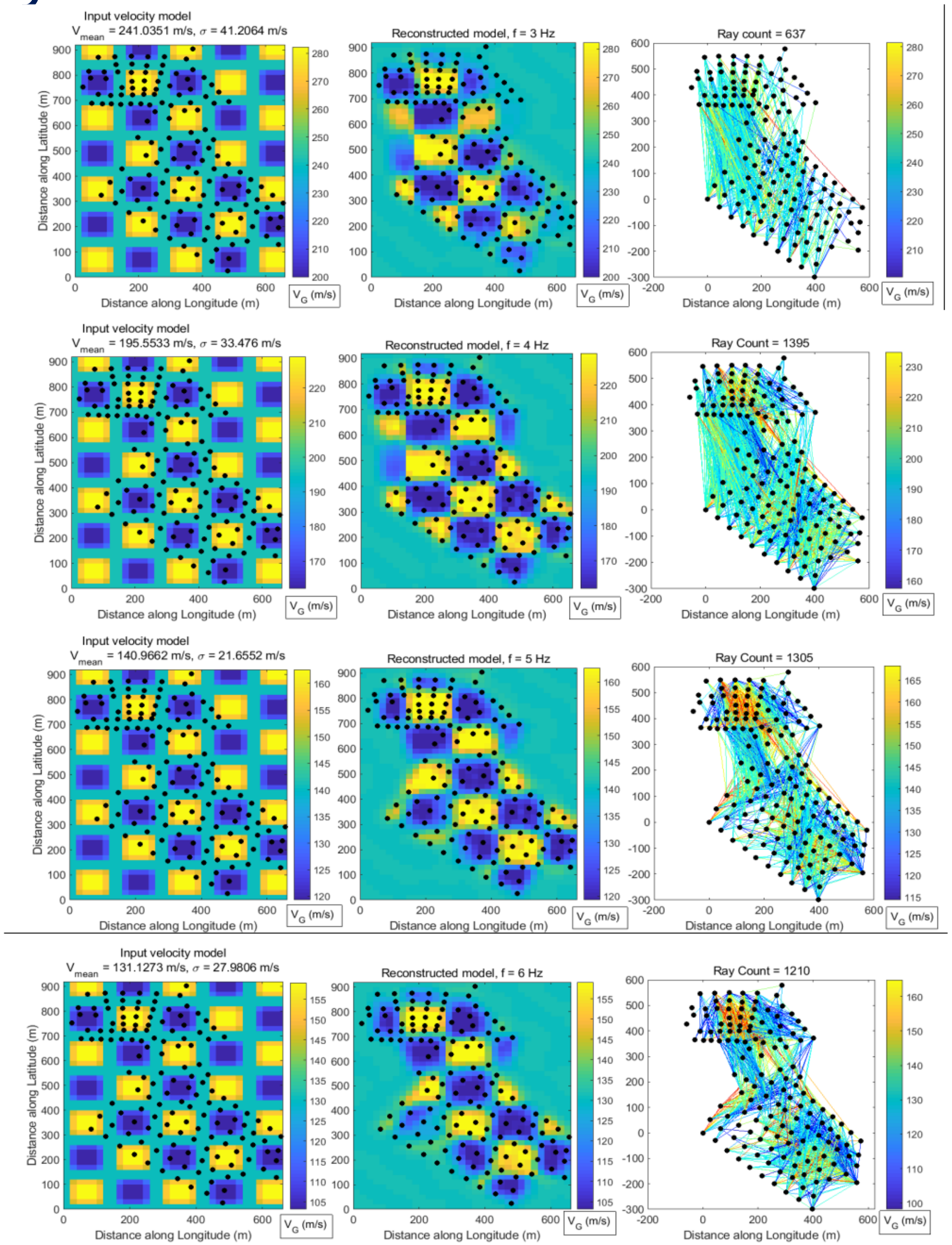

skoley@nikhef.nl

Passive seismic tomography *– Terziet Results*

Low frequencies between 3-3.4 Hz is sensitive to depths between 70-90 m, and high frequencies beyong 4.2 Hz are sensitive to changes in top 35 m of soft soil.

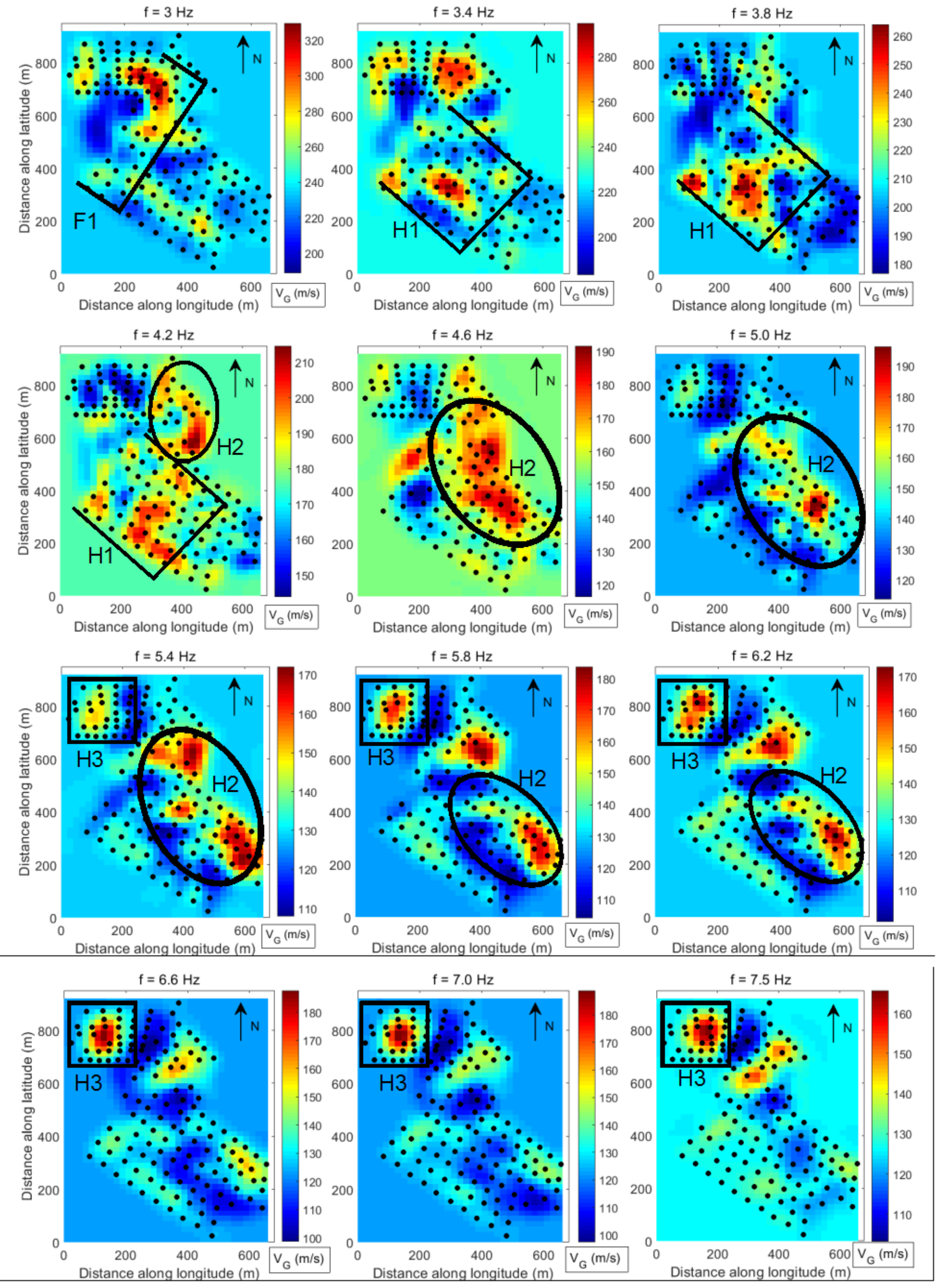

Interpretation:

- A overthrust fault in the region marked as F1 is characterized by a high velocity anomaly overlying a low velocity region.
- At high frequencies regions marked as H2 and H3 show a high velocity anomaly due to the presence of sandstone between the Vaals and the Namurien formation.
- The low velocity anomaly between H2 and H3 lack the presence of sandstone and was verifed from local excavations in the region.

skoley@nikhef.nl

Passive vs Active?

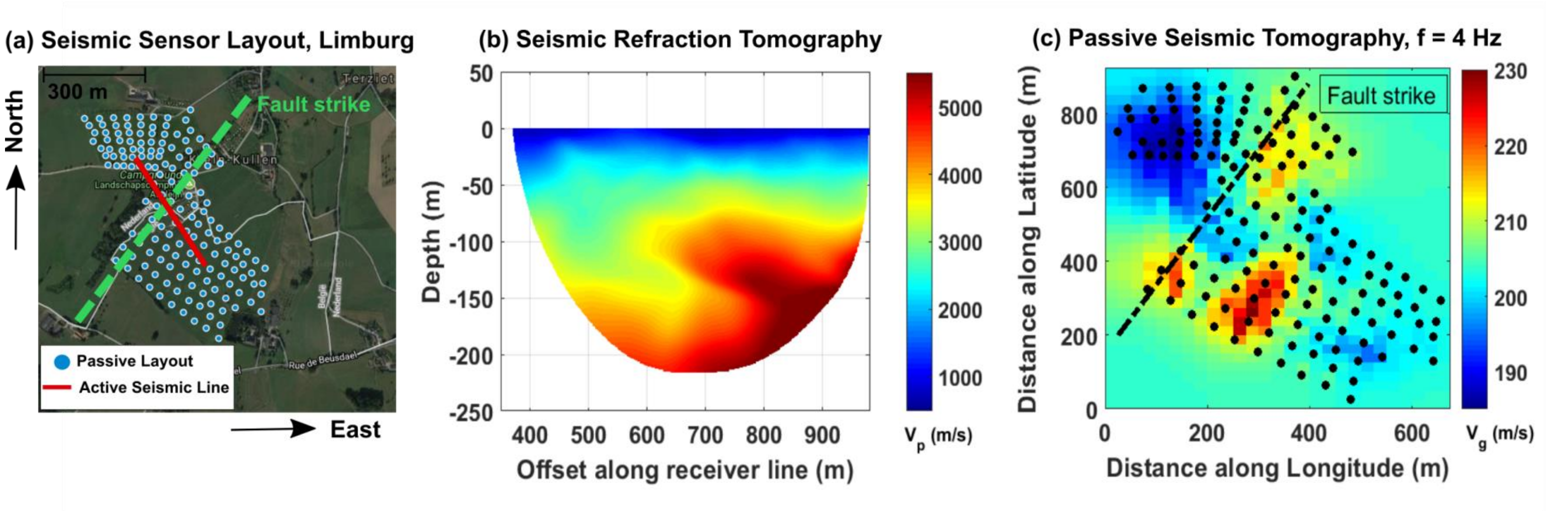

Figure 14. A comparitive plot showing the P-wave velocity depth model obtained using active seismic refraction method and the group velocity maps obtained from passive seismic analysis method. A high velocity anomaly characterizes the overthrust fault.

- We demonstrated the use of seismic noise for obtaining shallow S-wave subsurface models and which can be implemented near most GW detectors.
- These 3D models not only helps in better site characterization but also serves reliable computation of Newtonian noise.

Underground PSDs from simulated data

The simulations suggest a strong reduction of seismic amplitudes underground. This will be confirmed with a borehole study at the end of 2018

Underground PSD from synthetic data

- Below 2 Hz: Large Rayleigh wave amplitudes (>> 300m) lead to little attenuation factor underground
- Above 2 Hz: Attenuation of about one order of magnitude (in power) already at depth of 100 m with respect to surface
- This will be confirmed by borehole study to 300m depth planned for end 2018, with installation of 3-axial permanent seismic senor underground

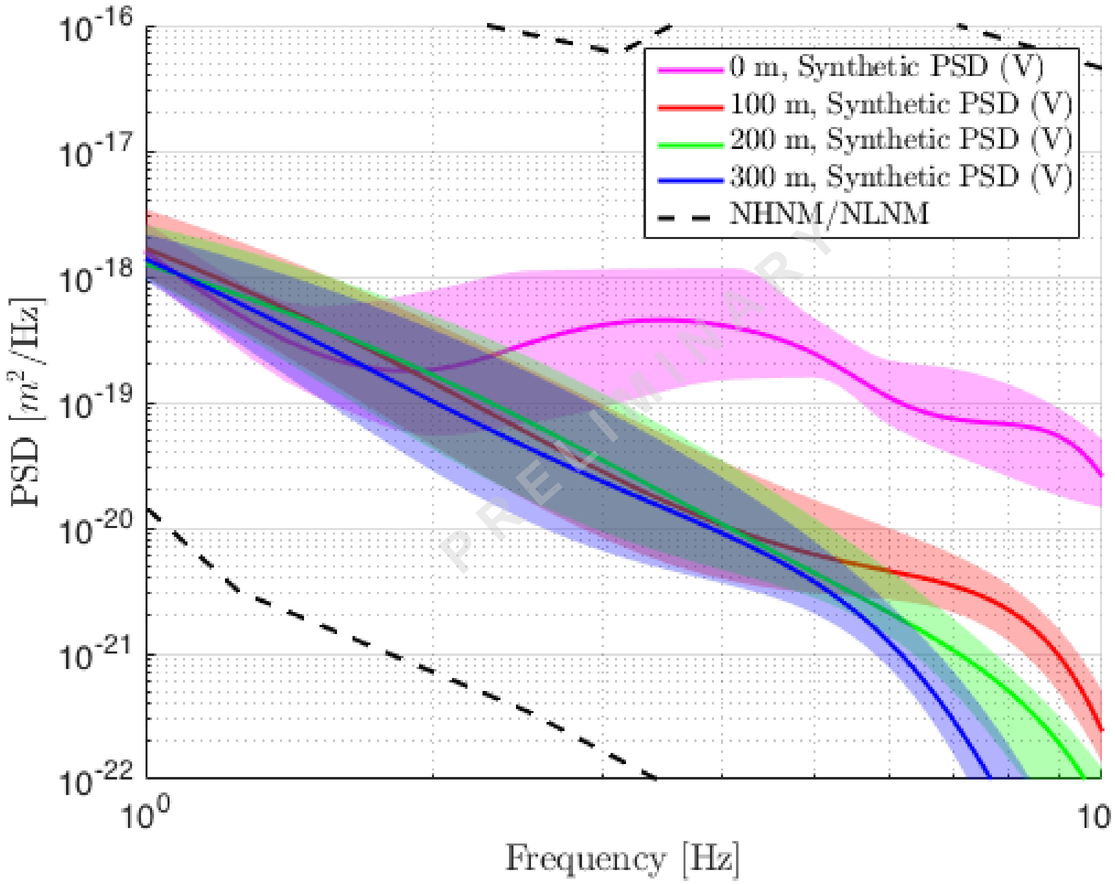

 Maria Bader, Soumen Koley

Newtonian noise depth at the ET candidate site

Newtonian noise underground is strongly suppressed with respect to surface Newtonian noise

Results

- Large reduction factor between surface and underground Newtonian noise achieved due to soft soil on hard rock geology
- Improvement from 100 m to 300 m due to increased distance to noisy surface layer
- Mean underground NN at 300 m drops ET design sensitivity curve
- Improved suppression can be achieved by subtraction schemes

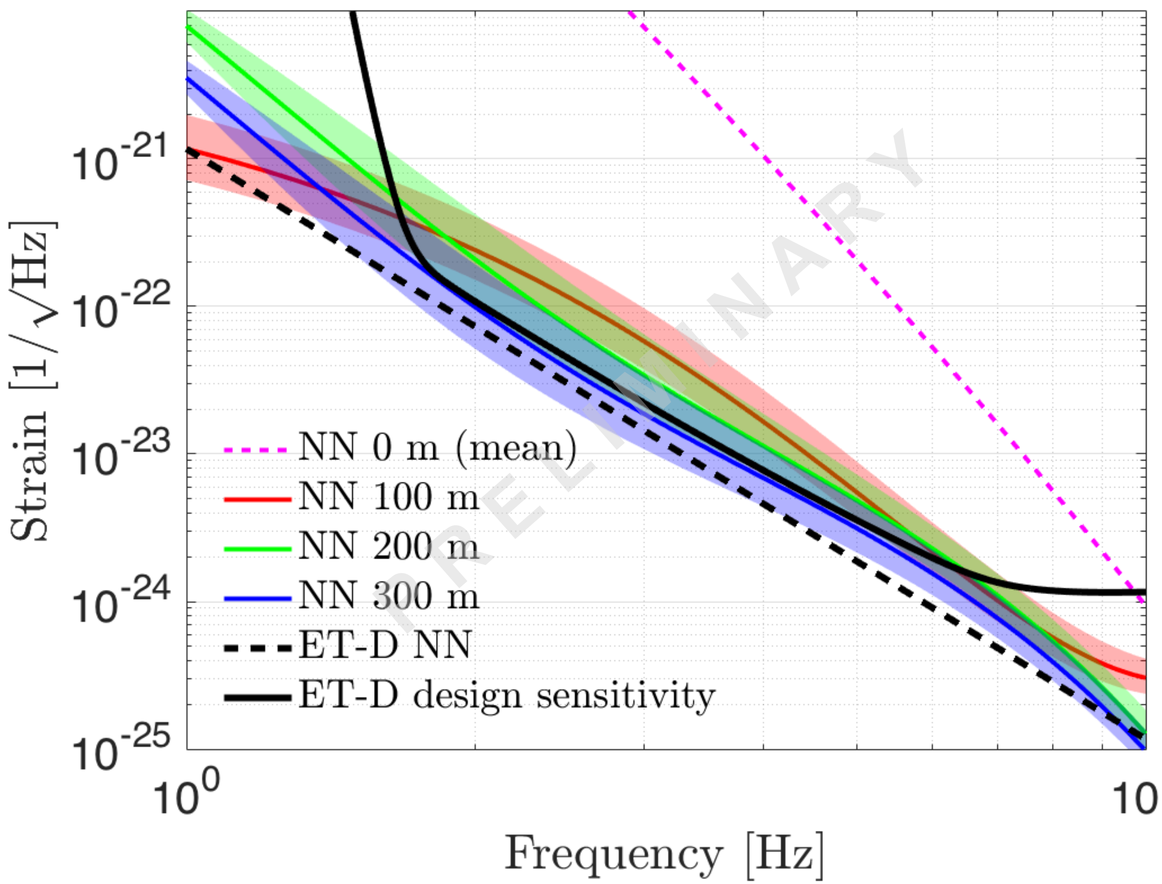

Conclusion & Outlook

- Currently a 260 m borehole is ready and seismometer to be installed between May 6 – 10, 2019.
- An accurate model of the subsurface to a depth of 260 m, Quality factor estimation to follow.
- Reliable calibration of underground seismic motion using the borehole seismometer data and hence better estimation of Newtonian noise.

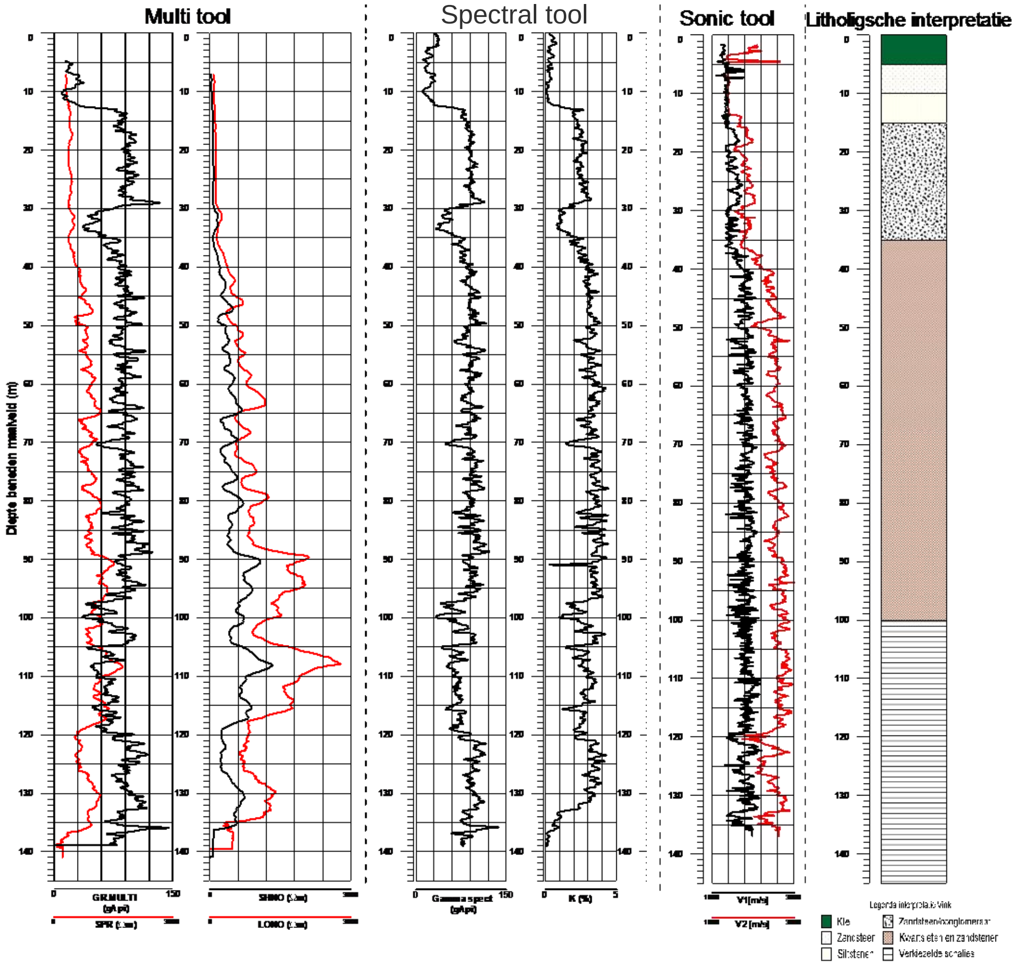

skoley@nikhef.nl


Questions?

References

- Processing seismic ambient noise data to obtain reliable broad-band surface wave dispersion measurements, G. D. Bensen[1], M. H. Ritzwoller[1], M. P. Barmin[1], A. L. Levshin[1], F. Lin[1], M. P. Moschetti[1], N. M. Shapiro[2] and Y. Yang. Geophysical journal International, 2007.
- On a frequency-time analysis of oscillations, A.L.Levshin, V.F. Pisarenko, G.A. Pogrebinsky, Annales of Geophysics, 1972.
- Surface wave tomography of the western United States from ambient seismic noise: Rayleigh and Love wave phase velocity maps, Fan-Chi Lin, Morgan P. Moschetti and Michael H. Ritzwoller, Geophysical Jounal International, 2007.
- A Comparison of Strategies for Seismic Interferometry, Roel Snieder, Masatoshi Miyazawa, Evert Slob, Ivan Vasconcelos, Kees Wapenaar, Survey Geophysics, 2009.
- Extracting the Green's function from the correlation of coda waves: A derivation based on stationary phase, Roel Snieder, Physical review E, 2004.
- Retrieving the Green's function in an open system by cross correlation: A comparison of approaches (L) Kees Wapenaar and Jacob Fokkema Department of Geotechnology, Delft University of Technology, Delft, The Netherlands Roel Snieder Center for Wave Phenomena, Colorado School of Mines, Golden, Colorado 80401, Acoustic Society of America, 2005.
- On measuring surface wave phase velocity from station–station cross-correlation of ambient signal, Boschi, Lapo; Weemstra, Cornelis; Verbeke, Julie; Ekström, Göran; Zunino, Andrea; Giardini, Domenico, Geophysical Journal International, 2012.
- Spectral Whitening in the Frequency Domain, M. W. Lee, Open-File Report 86-108, U.S Geological survey.
- A fast and reliable method for surface wave tomography, M.P. Barmin, M.H. Ritzwoller, A.L. Levshin, Pure and Applied Geophysics, 2001.
- Basic Principles of Wave Propagation, Gerard T. Schuster, 2011.

References

- High-resolution 3D shallow crustal structure in Long Beach, California: Application of ambient noise tomography on a dense seismic array, Fan-Chi Lin[1], Dunzhu Li[1], Robert W. Clayton[1], and Dan Hollis2, Geophysics, 2013.
- Case History: High-frequency Rayleigh-wave tomography using traffic noise from Long Beach, California Jason P. Chang[1], Sjoerd A. L. de Ridder[2], and Biondo L. Biondi[1], Geophysics, 2016.
- Surface-wave eikonal tomography for dense geophysical arrays Pierre Gouedard[1], Huajian Yao[1;2], Fabian Ernst[3], and Robert D. van der Hilst[1,] [1]Earth, Atmospheric and Planetary Sciences department, Massachusetts Institute of Technology, [2]Institute of Geophysics and Planetary Physics, Scripps Institution of Oceanography, [3]Shell Projects and Technology.
- Rayleigh wave group velocities at periods of 6–23 s across Brazil from ambient noise tomography Bruno Goutorbe,[1] Diogo Luiz de Oliveira Coelho[2] and St´ephane Drouet[2], Geophysical Journal International, 2015.
- Passive seismic imaging with directive ambient noise: application to surface waves and the San Andreas Fault in Parkfield, CA, Philippe Roux, Geophysical Journal International, 2009.
- Tomographic inversion via the conjugate gradient method John A. Scales*, Geophysics, 1987.
- Traveltime tomography: A comparison of popular methods, W. Scott Phillips* and Michael C. Fehler, Geophysics, 1991.
- Shaping regularization in geophysical-estimation problems, Sergey Fomel1, Geophysics, 2007.
- On the effect of topography on surface wave propagation in the ambient noise frequency range Andreas Köhler · Christian Weidle · Valérie Maupin, Journal of Seismology, 2011.